Phosphating modification with metal ions of carbon steel surface to improve the influence of anticorrosion properties

Samardžija, Marina; Alar, Vesna; Špada, Vedrana; Kapor, Frankica

Source / Izvornik: **Technologies, 2021, 10**

Journal article, Published version
Rad u časopisu, Objavljena verzija rada (izdavačev PDF)

https://doi.org/10.3390/technologies10010003

Permanent link / Trajna poveznica: https://urn.nsk.hr/urn:nbn:hr:169:092899

Rights / Prava: Attribution 4.0 International/Imenovanje 4.0 međunarodna

Download date / Datum preuzimanja: **2024-04-25**

Repository / Repozitorij:

Faculty of Mining, Geology and Petroleum Engineering Repository, University of Zagreb

DIGITALNI AKADEMSKI ARHIVI I REPOZITORIJI

technologies

MDPI

Article

Phosphating Modification with Metal Ions of Carbon Steel Surface to Improve the Influence of Anticorrosion Properties

Marina Samardžija [1,*], Vesna Alar [2], Vedrana Špada [3] and Frankica Kapor [1]

[1] Department of Chemistry, Faculty of Mining-Geology-Petroleum Engineering, University of Zagreb, 10110 Zagreb, Croatia; frankica.kapor@rgn.hr
[2] Department of Welded Structures, Faculty of Mechanical Engineering and Naval Architecture, University of Zagreb, 10000 Zagreb, Croatia; vesna.alar@fsb.hr
[3] Center of Material Research, Università Istriana di Scienze Applicate, METRIS Research Centre Pula, 52100 Pula, Croatia; vspada@iv.hr
* Correspondence: marina.samardzija@rgn.hr; Tel.: +385-1-5535-912

Abstract: The purpose of this research is to investigate the influence of the phosphatizing process with Ni^{2+}, Ce^{3+}, and Ti^{2+} ions on the properties of the coating to obtain better corrosion protection of the metal. Steel corrosion occurs through physicochemical interaction between the metal and its surrounding environment. This leads to a change in the metal's physical, mechanical, and optical properties that can cause damage to the functionality of the metal, which in turn may result in accidents or other malfunctions. Carbon steel grade has limited resistance to corrosion, depending on the carbon content and alloying element, the microstructure, and the surrounding environment of the material. This paper present tests that have been carried out on some of the physicochemical properties of protective epoxy and polyurethane coating on carbon steel grade. Coatings represent one of the methods available to protect metal surfaces from corrosion. Coating properties such as thickness, hardness, and adhesion were investigated. The same properties were tested by exposing the sample plates to corrosive conditions of the humid chamber and seawater. Their anticorrosion properties were explored by electrochemical impedance spectroscopy (EIS) techniques under immersion in 3.5 wt.% NaCl solutions as a corrosive medium. Part of the samples prior to application of the coatingwere modified with a phosphate solution containing metal ions: Ni^{2+}, Ce^{3+}, and Ti^{2+} to further investigate the effects of phosphatization on the properties of the coating. After exposure of the plates to the salt and moist chamber conditions, no traces of corrosion products, cracking or peeling of the coating were found on the surfaces. The adhesion properties were tested by the pull-off adhesion test. It was found that metal/polymer adhesion was satisfied according to EN ISO 4624:2016 and had the same value for all samples. However, a detailed EIS analysis showed a higher resistance of phosphate samples with Ce^{3+} ions than samples that were phosphated with Ni^{2+} and Ti^{2+} ions and those that did not have a sparingly soluble phosphate salt layer.

Keywords: corrosion resistance; phospatization; coating; carbon steel; nickel; cerium; titan

check for updates

Citation: Samardžija, M.; Alar, V.; Špada, V.; Kapor, F. Phosphating Modification with Metal Ions of Carbon Steel Surface to Improve the Influence of Anticorrosion Properties. *Technologies* **2022**, *10*, 3. https://doi.org/10.3390/technologies10010003

Academic Editor: Manoj Gupta

Received: 26 November 2021
Accepted: 24 December 2021
Published: 28 December 2021

Publisher's Note: MDPI stays neutral with regard to jurisdictional claims in published maps and institutional affiliations.

Copyright: © 2021 by the authors. Licensee MDPI, Basel, Switzerland. This article is an open access article distributed under the terms and conditions of the Creative Commons Attribution (CC BY) license (https://creativecommons.org/licenses/by/4.0/).

1. Introduction

Iron and iron alloys, including non-alloyed ones, are popular in the design and construction of engineering structures and piping applications [1,2]. Unfortunately, the mechanical properties, of non-alloy steels, including surface hardness, are not outstanding, and their use is restricted in certain applications [3]. Any heat treatment or other thermal process that takes the alloy too far from the nominal phase balance, or introduces third phases, can result in reduced mechanical properties, corrosion resistance, or both [4]. However, the environments to which they are deployed cause not only damages, but also produce great waste of resources and economic losses [1,5]. Steel is very sensitive to different forms of corrosion, especially when used in harsh environments such as the oil and gas industry. However, appropriate corrosion methods can help avoid many

potential disasters that can cause serious issues including loss of life, negative social impacts, pollution of water resources, and environmental pollution [2,6]. Apart from the oil and gas sector, the marine environment is one of the most aggressive working environments where structural materials and components are exposed to high levels of chloride, oxygen, and other corrosive minerals, in addition to the seawater spray arising from the ship motion and wave effects [2,7,8].

The application of organic coatings on steel surfaces is a promising strategy for extending their service life, although they are all permeable to moisture and oxygen. To overcome these problems, there is a growing tendency to apply thicker coatings for marine conditions [9,10]. Organic coatings, such as polyester, epoxy, polyurethane resins, provide a passive physical barrier between the corrosive environment and the metal surface [9,11]. Among these organic coatings, epoxy coatings are the most broadly applied type of coatings for industrial and engineering applications due to their advantages of good protection, simple application method, good adhesion to metals, high corrosion resistance and low cost [5,12,13]. These coatings include an inner primer layer loaded with anti-corrosion pigments [2]. The topcoat provides the main protection from environmental hazards and enables different functional and aesthetic applications. An intermediate coating sometimes needs to be added to increase the total coating system thickness and enhance thebarrier effect against highly corrosive environments [10,14].

According to ISO 12944-2 [15], there are five corrosivity categories ranging from C1 to C5, where C5 stands for a very high corrosion risk. Moreover, the environment is classified also according to immersion category ranging from Im1 to Im4. However, after long exposure periods, the absorbed water, oxygen, and corrosive ions can diffuse into the epoxy resin through coating defects derived from improper curing, low cross-link density, and local shrinkage resulting in coating delamination (adhesion loss) and substrate corrosion [16]. To enhance corrosion protection, surface treatment and various coatings have been suggested and applied [17].

A thin phosphate coating was used to investigate its influence as an adhesion promoter [18]. The phosphatizing process is the most widely used metal pre-treatment process, which involves a topochemical reaction between a primary phosphate solution with a metal surface, promoting the precipitation of an insoluble tertiary salt [18,19]. This process is the most common type of chemical treatment, which has been primarily used as a pre-treatment to protect surfaces against underpaint corrosion, to pre-treat surfaces for metal forming operations, such as cold extrusion, and to improve corrosion resistance by providing a good base for waxes and rust-preventive oils [20]. Due to its economy, speed of operation, and ability to afford excellent corrosion resistance, wear resistance, adhesion, and lubricative properties, it plays a significant role in the automotive, processing, and appliance industries [21,22]. Metal coatings also provide good benefits against early rusting but decrease the grade of steel in practical application [23]. Epoxy coating can protect the metal substrate by releasing inhibiting chemicals from the pigment to form a strong passive or barrier layer that inhibits the corrosive medium contact with the metal substrate [24]. So far, the classical alternative, zinc phosphate, has been widely used [25].

In this paper, a three-layer coating system was applied to different pre-treatment carbon surfaces to determine which surface has better resistance to corrosion. However, the present work explores the influence of introduced cerium, nickel, and titan on the zinc phosphate pre-treatment. The effect of phosphated surface was evaluated in different aggressive media, such as humidity chamber and immersion in 3.5% NaCl solution. In addition, the results of morphology, thickness, hardness, RAL colors, adhesion straight, and EIS measurements are presented in this study.

2. Materials and Methods

2.1. Material

The materials used in this study include epoxy coating and polyurethane. In this study carbon steel was investigated. The chemical composition of the carbon steel is shown in Table 1.

Table 1. The chemical composition of the carbon steel sample was determined by optical emission spectrum GDS 850 A, LECO.

Element	C	Si	Mn	P	S	Cr	Mo	Ni	Cu	Fe
Percent (%)	0.33	0.16	0.55	0.019	0.019	0.06	0.01	0.03	0.04	balance

2.2. Substrate Pre-Treatment

2.2.1. Modification of the Phosphate Film by Ni^{2+}, Ce^{3+} i Ti^{2+} Ions

Common carbon steel plates of 3 mm thickness were cut into pieces of 100 × 150 mm. Before applying the coating, part of the samples was modified with a phosphate solution which were containing metal ions: Ni^{2+}, Ce^{3+}, and Ti^{2+}.

In the first stage, the surfaces of samples were cleaned with abrasive blasting to remove surface contaminants. This kind of process also shapes the surface and gives it satisfactory roughness. In the second stage, four tanks (Legor Group S.P.A., Bressanvido, Italy) were used for phosphatizing. Table 2 shows the composition of the baths used for surface modification of carbon steel.

Table 2. Bath compositions and deposition parameters.

Bath	Bath 1	Bath 2	Bath 3	Bath 4
H_3PO_4, mL/L	14	14	14	14
ZnO, g/L	12	12	12	12
HNO_3, mL/L	12	12	12	12
$NaNO_2$, g/L	2	2	2	2
NaOH, g/L	3	3	3	3
$NiSO_4 \cdot 7H_2O$, g/L	-	1.25	-	-
$CeCl_3$, g/L	-	-	1.25	-
TiO_2, g/L	-	-	-	1.25
Temperature, °C	70	70	70	70
Duration, min	15	15	15	15

After phosphatizing, allthe samples were cleaned with water.

2.2.2. Preparing of Coating System with Modified Phosphate Surface

The obtained surface modifications by Ni^{2+}, Ce^{3+}, and Ti^{2+} ions have been protected by the coating system shown in Table 3.

Table 3. Preparation of three-layer coating system on carbon steel substrate.

Coat	Binder	Solvent
primer coat	epoxy resin	xylene, but-1-ol and toluene
intermediate coat	epoxy resin	xylene, but-1-ol and toluene
topcoat	polyurethane	n-butil-acetat, petrol

The primer and the intermediate coats contained a two-component Bisphenol-A type epoxy resin. In this regard, the epoxy/solvent was mixed with xylene, but-1-ol and toluene by a mass ratio of 132:18. Finally, the polyurethane was used as a topcoat. The obtained mixtures were applied to the steel panels by a film applicator (coating thickness: 100 μm). The primer coat was cured with an infrared radiation at 60 °C for 15 min while

the intermediate and the top layers were dried at room temperature for 24h. Eight samples were prepared for corrosion measurements: four samples were phosphatized (Table 4) and the other four were not phosphatized.

Table 4. Modified phosphatized samples protected by the coating system.

Samples	Phosphating Solution Modified with	Three-Layer Coating System
Sample 1	-	primer, intermediate and topcoat
Sample 2	Ni^{2+} ions	primer, intermediate and topcoat
Sample 3	Ce^{3+} ions	primer, intermediate and topcoat
Sample 4	Ti^{2+} ions	primer, intermediate and topcoat

2.3. Surface Analysis Techniques

The morphology of the phosphate steel surface and steel surface phosphated with Ni^{2+}, Ce^{3+}, and Ti^{2+} ions and protected with organic coating was observed by using a scanning electron microscopy (SEM) (TESCAN Brno, Brno, Czech Republic) at a magnification of 100× and by a stereo microscope model Leica MZ6 (Leica Microsystems, Heebrugg, Switzerland) at a magnification of 50×. Additionally, phosphate steel surface and phosphate surface with Ni^{2+}, Ce^{3+}, and Ti^{2+} ions were examined by SEM with the addition of energy dispersive X-ray (EDS) spectroscopy for elemental composition analysis. The surface roughness of samples, as substrates for epoxy coating deposition, was determined by Surface Roughness Tester (model: TMR200). RAL colors (RAL gGmbH, Siegburger, Germany) were used for defining standard colors of coating. A coating thickness gauge Elcometer® 456 (Elcometer Limited, Edge Lane, Manchester, UK) was used to assess the thickness of the coated samples. Measurements were performed on ten different locations per sample. The testing of the coating hardness was performed according to the EN ISO 15184 standard [26]. The testing was performed using the Elcometer gauge, model 161 (Elcometer Limited, Edge Lane, Manchester, UK). Using pencils of different hardness, from 9B to 9H, the coating hardness was measured. The pencils were posi-tioned at a 45-degree angle, whereas the loading force was 7.5 N. To investigate the adhesion strength between the epoxy coating and the substrate, a PosiTest Pull-off Adhesion Tester (Elcometer Limited, Manchester, UK) was conducted. Elcometer Cyanoacrylate Adhesive was used for aluminum dollies with a diameter of 20 mm, and it was dried at room temperature for 24 h. To validate the repeatability of the results, measurements were performed on each sample several times. Adhesion properties were tested immediately after drying and after exposure to corrosion conditions.

In this paper, accelerated laboratory tests to predict the corrosion performance of the phosphate and phosphate steel surface modified with Ni^{2+}, Ce^{3+}, and Ti^{2+} ions were used. The Machu test was performed on samples immerged in the solution for 48 h which is equivalent to a 1000-h exposure in salt chamber. The solution for the Machu test in which the samples were immersed was made of 50 g/L NaCl, 10 g/L CH_3COOH, 5 g/L H_2O_2 (30% solutions) and deionized water. The pH-value of the solution was 3 [27]. The samples were immersed in 3.5 wt.% NaCl solution in a glass jar for 48 h which corresponds to a 1000-h exposure in salt chamber test. Moreover, the humidity test was conducted according to EN ISO 6270-2 in which the samples were exposed for seven days [28]. The accelerated testing was performed on two samples per coating.

Electrochemical impedance spectroscopy (EIS) was carried out on phosphated sample, phosphated samples with Ni^{2+}, Ce^{3+}, and Ti^{2+} to determine the best corrosion resistance. The phosphated sample (with Ce^{3+} ions) and the phosphate steel surface protected with a three-layer coating system were measured. For this purpose, VersaSTAT 3 Potentiostat/Galvanostat (AMETEK Scientific 131 Instruments, Princeton applied research, Berwyn, PA, USA) was used. The experiment was conducted at open circuit potential (OPC) with the frequency range from 100 kHz to 100 mHz and amplitude perturbing signal of 10 mV. The measurements were carried out, respectively, after one hour and after 7 days of immersion

in 3.5 wt.% NaCl solution, pH = 7.554, at room temperature (20 ± 2) °C which is the closest to the marine environment and is widely used for corrosion tests [2]. A three-electrode set-up in an electrochemical cell, where Pt sticks served as the auxiliary electrodes, a saturated calomel electrode (SCE) as the reference electrode and a phosphate and coated steel sample as a working electrode with exposed surface area of 1.0 cm^2 (without defect). Each measurement was implemented in three replications for checking the repeatability of data. The ZSimWin software was used to interpret data.

3. Results and Discussion

3.1. Surface Morphology of Carbon Steel

Figure 1a–d shows the top view image of the phosphate steel surface and phosphate steel surface which were modified with Ni^{2+}, Ce^{3+}, and Ti^{2+} ions. According to Bajat [18], phosphate coating may absorb oil, wax, or pain very well, so this is one of the indicators that the bonding ability between the surface and the coating has been improved. Moreover, a thin layer of iron oxide formed on the bare steel surface thus improving the air resistance of the material. Theoretically, phosphatization can better protect the surface from oxide or nitrogen due to this thin layer which contains insoluble phosphate salts.

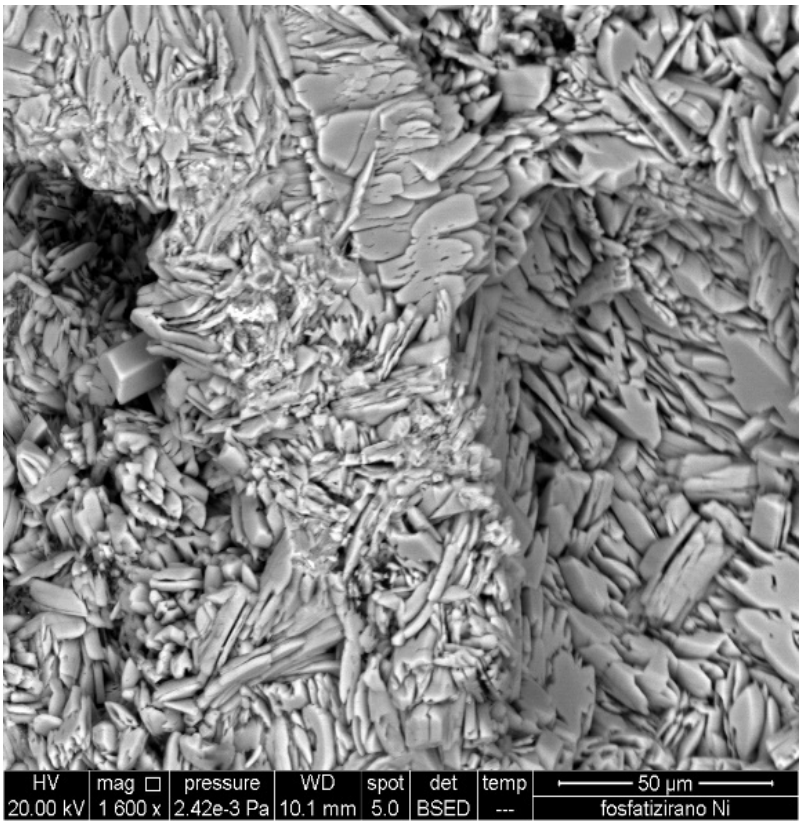

(**a**)

Figure 1. *Cont.*

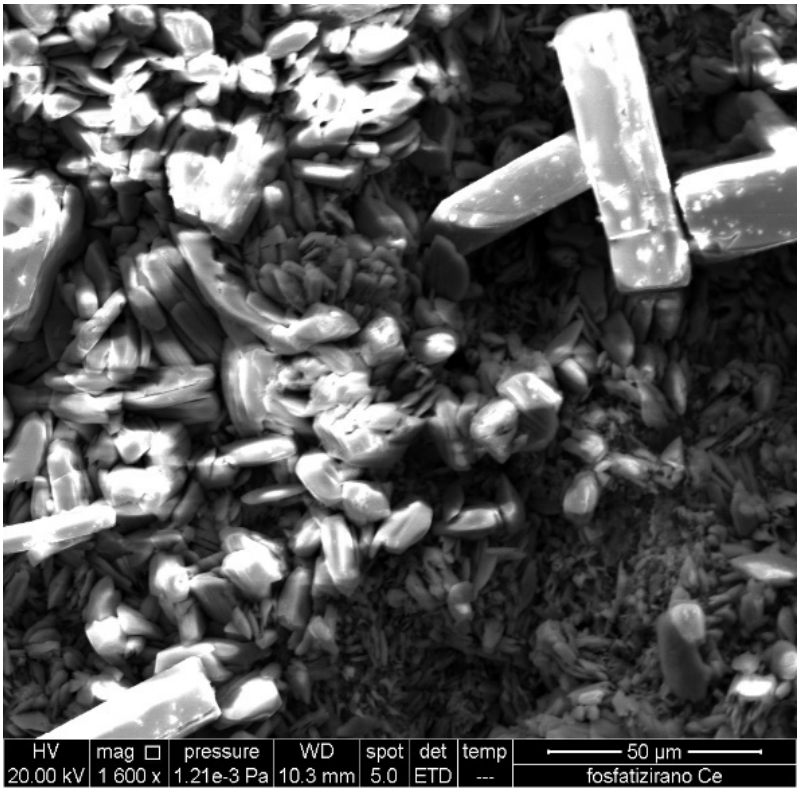

(**b**)

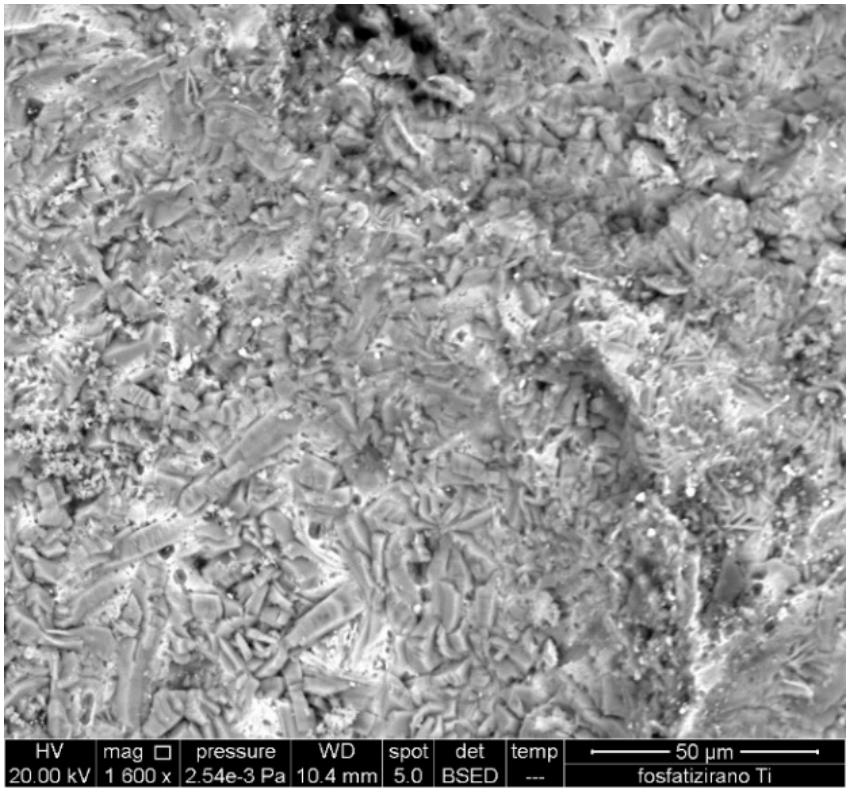

(**c**)

Figure 1. SEM micrographs phosphating carbon steel surface with Ni^{2+} ions (**a**), Ce^{3+} ions (**b**) and with Ti^{2+} ions (**c**).

The influence of Ni^{2+}, Ce^{3+}, and Ti^{2+} ions on the carbon steel surface is shown in Figure 1a–c. The distribution of carbon is visible at large magnifications. In the presence of the phosphate solution, the samples show a uniform grain microstructure of scales or needles. In addition, these phenomena indicate that the molecule of zinc phosphate was absorbed on the surface of carbon steel to form a protective film, which prevented the contact between the surface of carbon steel and acid and, as a result, reduced corrosion. In contrast to the Zn coating, Ni^{2+}, and Ce^{3+} ions formed needle crystals on the surface, indicating an easier adhesion of these ions to the surface.

Figure 2 illustrates the morphology and the local chemical composition of the phosphate samples with Ni^{2+}, Ce^{3+}, and Ti^{2+} ions.

The elemental mapping by EDS spectroscopy (Figures 2 and 3) for samples showed the presence of Fe, P, and O ions suggesting that an iron phosphate compound was generated at the beginning of the phosphatizing process [19]. The chemical composition of all samples revealed a high concentration of zinc ions. EDS results displayed in Figure 2a clarified that the phosphate coating included 0.27 wt.% of Ni^{2+} ions. Ni ions catalyze the process of phosphate film formation on the steel surface. Orthorhombic Ni crystals on the surface of the phosphate film contribute to good adhesion of the film to the substrate's surface.

The addition of Ce^{3+} ions in the phosphate bath resulted its appearance of 27.10 wt.%. Ce ions from the solution are reduced and deposited on the phosphate film, they inhibit the film and affect the growth of the phosphate film grains. The action of Ce^{3+} ions is also demonstrated in the reduction of structural inefficiencies such as porosity and cracking.

According to Figure 2c, the steel surface contains 0.09 wt.% Ti^{2+} ions. These ions affect the morphology of the layer. The evidence of other metals on the carbon steel surface was confirmed by EDS mapping (Figure 3). Figure 3f shows a significant amount of cerium ions compared to the other elements. All subsequent experiments were made on the phosphate surface with Ce^{3+} ions.

The surface qualities on which the roughness measurement was proven differed primarily in the appearance of the surface. The thickness of the phosphate layer was measured with Elcometer® 456 and is shown in Table 5.

According to Table 6, it can be concluded that there is no difference in roughness between the phosphated and the modified phosphated samples. It is obvious from these results that the roughness is the same because all the samples had been prepared with abrasive blasting. Assessingthe surface in both samples shows medium category according to ISO 8503-1 [29]. This roughness did not consume a large amount of paint and consequently, it did not increase the costs.

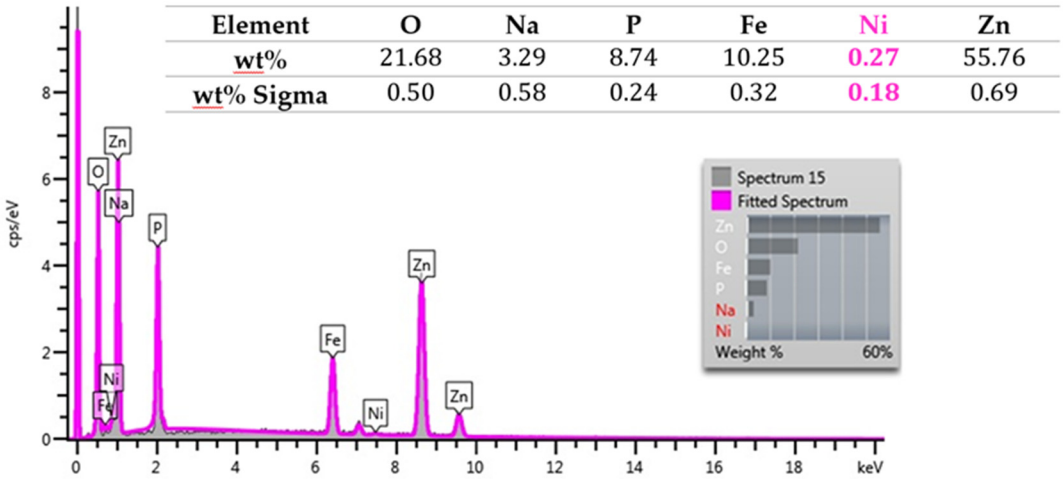

Element	O	Na	P	Fe	Ni	Zn
wt%	21.68	3.29	8.74	10.25	0.27	55.76
wt% Sigma	0.50	0.58	0.24	0.32	0.18	0.69

(**a**)

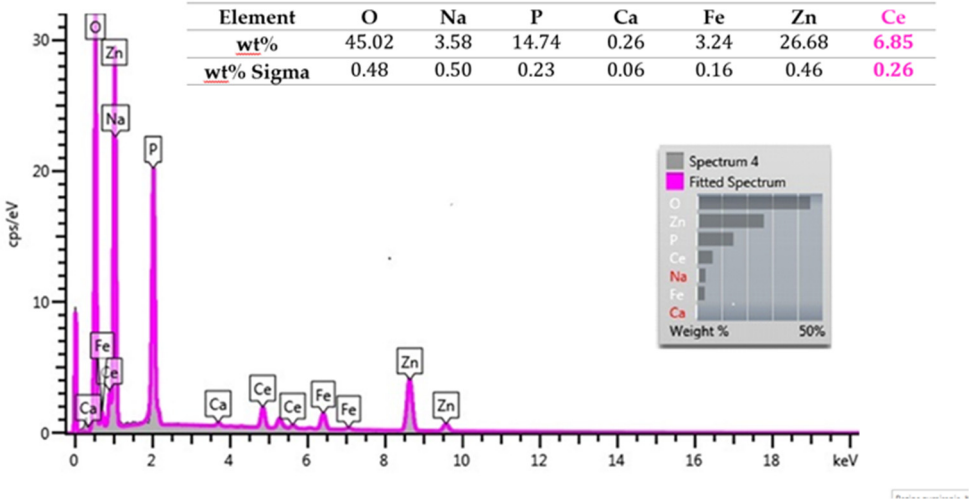

Element	O	Na	P	Ca	Fe	Zn	Ce
wt%	45.02	3.58	14.74	0.26	3.24	26.68	6.85
wt% Sigma	0.48	0.50	0.23	0.06	0.16	0.46	0.26

(**b**)

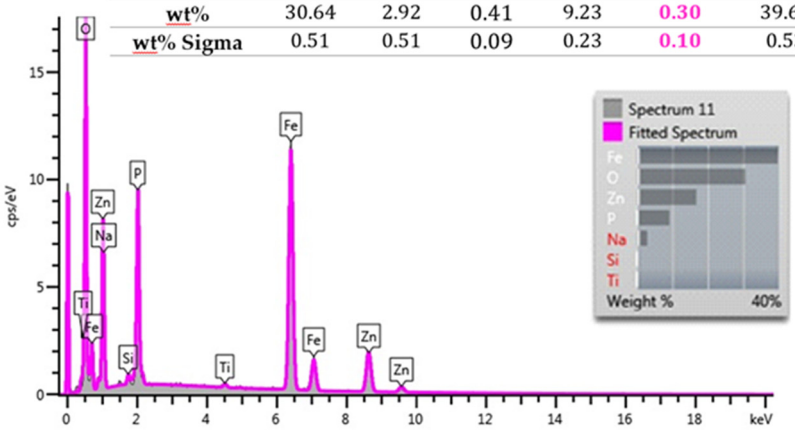

Element	O	Na	Si	P	Ti	Fe	Zn
wt%	30.64	2.92	0.41	9.23	0.30	39.66	16.84
wt% Sigma	0.51	0.51	0.09	0.23	0.10	0.53	0.53

(**c**)

Figure 2. EDS analysis obtained from the surface of phosphate coatings with different pre-treatments processes: (**a**) Ni^{2+} ions, (**b**) Ce^{3+} ions, and (**c**) Ti^{2+} ions.

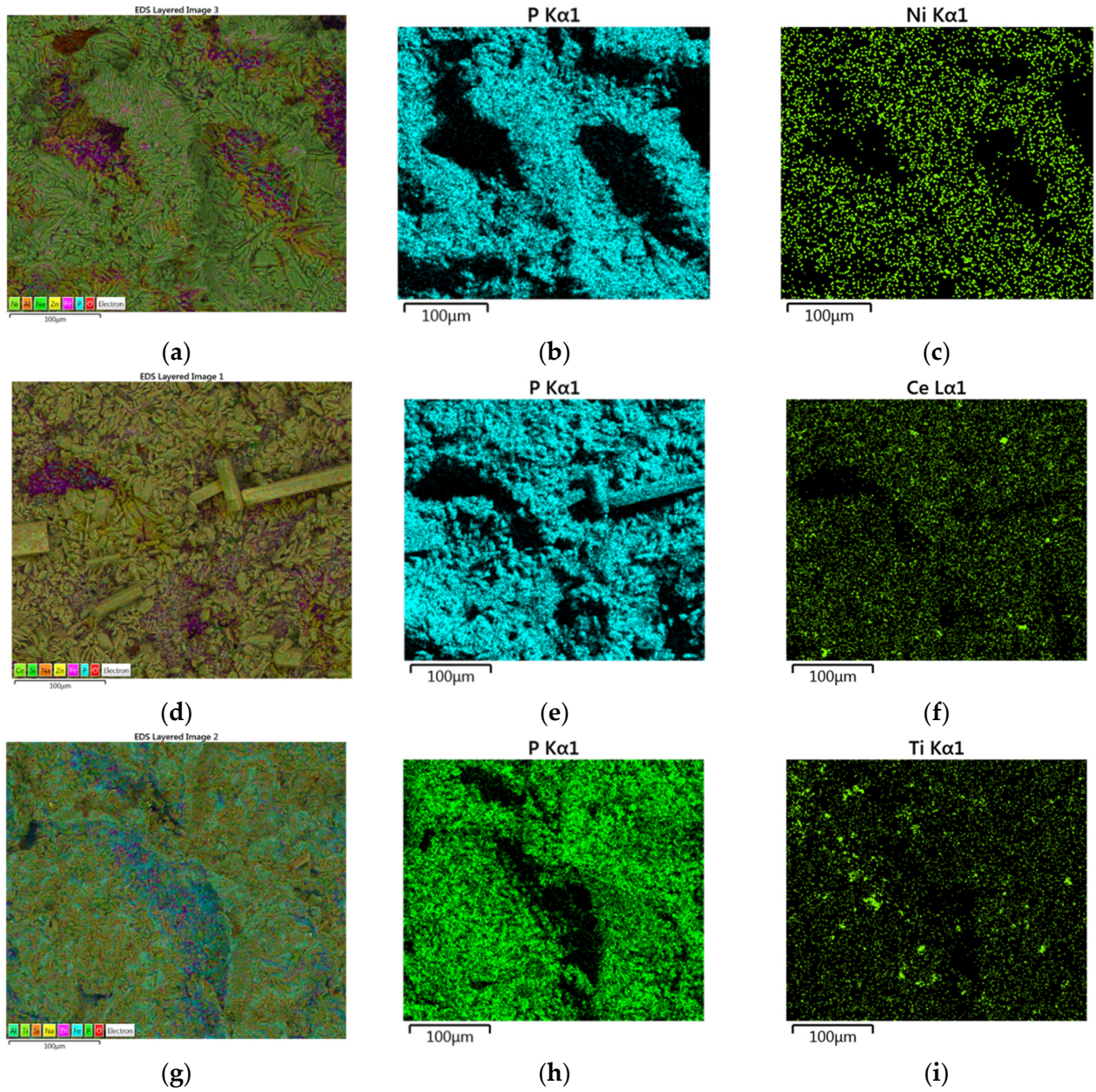

Figure 3. The SEM micrograph displays area analyzed phosphate layer with (**a**) Ni^{2+} ions, (**d**) Ce^{3+} ions and (**g**) Ti^{2+} ions. EDS mapping for (**b**,**e**,**h**) phosphorus distribution and distribution of (**c**) layers Ni^{2+} ions, (**f**) Ce^{3+} ions and (**i**) Ti^{2+} ions on phosphate steel plates.

Table 5. The value of thickness for phosphate sample and phosphate samples with Ni^{2+}, Ce^{3+}, and Ti^{2+} ions.

	Phosphate Sample	Phosphate Samples with Ni^{2+}	Phosphate Samples with Ce^{3+}	Phosphate Samples with Ti^{2+}
Thickness (µm)	15.03	15.92	21.69	14.01

Table 6. The values of surface roughness for phosphate sample and phosphate samples with Ni^{2+}, Ce^{3+}, and Ti^{2+} ions.

Samples	Phosphate Samples	Phosphate Samples with Ni^{2+}	Phosphate Samples with Ce^{3+}	Phosphate Samples with Ti^{2+}
R_z (μm)	53.29	50.63	55.86	51.49
R_a (μm)	8.70	8.91	9.25	9.03

3.2. Modification of the Phosphate Film by Ce^{3+} Ions

Further studies of corrosion resistance have been conducted on the phosphate film modified by Ce^{3+} ions. EDS analysis shows that the share of Ce^{3+} ions in the phosphate film compared to Ni and Ti ions is significantly higher. Ce^{3+} ions are incorporated into the phosphate film following the same mechanism as Zn^{2+} ions. Table 7 shows the logarithm of the dissociation constant, log *K*, for salts that the Ce^{3+} ion may form with H_3PO_4.

Table 7. Logarithm of dissociation constant for Ce^{3+} salts formed with residues of phosphoric acid. [30].

Reaction	log *K*
$Ce^{3+} + H_2PO_4^{-} \rightarrow CeH_2PO_4^{2+}$	−2.43
$Ce^{3+} + HPO_4^{2-} \rightarrow CeHPO_4^{+}$	−4.98
$Ce^{3+} + 2HPO_4^{2-} \rightarrow Ce(HPO4)_2^{-}$	−8.34
$Ce^{3+} + PO_4^{3-} \rightarrow CePO_4$	−11.35
$Ce^{3+} + 2PO_4^{3-} \rightarrow Ce(PO_4)_2^{3-}$	−18.48

According to dissociation constant logarithms, log *K*, from Table 7, it can be concluded that primarily cerium (III) phosphate will bind to the greatest extent to the carbon steel surface given the low value of log *K*. The main reactions were formation of a zinc and cerium phosphate film on the metal surface and the release of hydrogen [31]. The conventional view of the phosphate process with zinc ions is that following reaction occur [32]:

$$3Zn^{2+} + 2H_2PO_4^{-} + 2H^{+} + 4H_2O + 6e^{-} \rightarrow Zn_3(PO_4)_2 \cdot 4H_2O\downarrow + 3H_2\uparrow \quad (1)$$

The Fe^{2+} ions, which are in steel surface, also do react with acid radicals PO_4^{3-}. The following is the reaction [33]:

$$3Fe + 2H_3PO_4 \rightarrow Fe_3(PO_4)_2 + 3H_2\uparrow \quad (2)$$

3.3. Coating Thickness Measurement

The thickness of the dried coatings is shown in Figure 4. A similar value was measured for all three layers of coatings. The primer coat on the phosphate samples modified with Ce^{3+} ions, shows a slight increase in thickness compared to the phosphated carbon surface. In any way, these results confirm uniformly applied layers because the minimum (L_o) and the maximum (H_i) thickness of all coatings do not deviate significantly. The average coating thickness was about 250 μm.

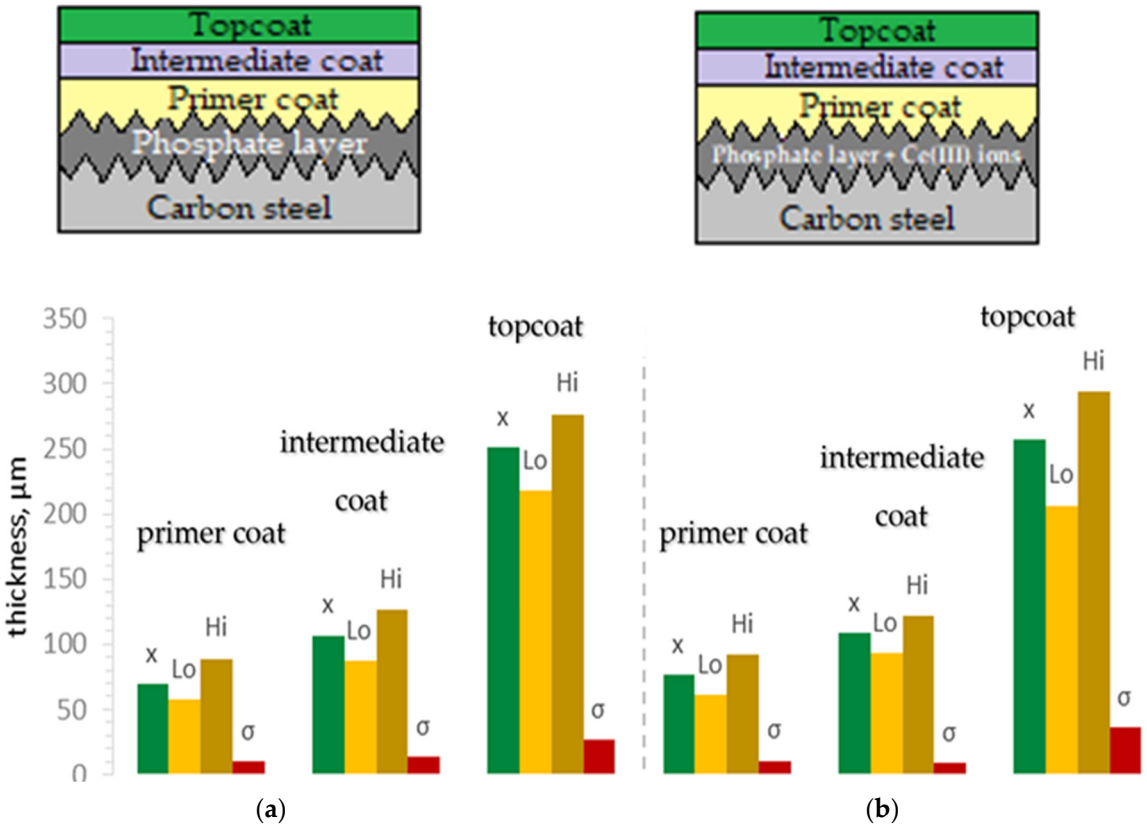

Figure 4. Scheme of steel samples with phosphate layer and three-layer epoxy coating. Parameters of thickness for applied primer, intermediate coat, and topcoat on (**a**) phosphated and (**b**) phosphate samples with Ce^{3+} ions.

3.4. Accelerated Corrosion Tests

Coating steel samples were exposed to a humidity (ISO 6270-2) chamber and immersed in a 3.5% solution of NaCl (ASTM B117) to compare their physical properties and corrosion behavior [28,34]. After exposure of the plates to the accelerated corrosion tests, no traces of corrosion products, cracking, or peeling of the coating were found on the surface.

Physical properties, including color and hardness, were observed immediately after the application of the coating and after 23 days. We found that the standard color of polyurethane, gray with a bright metallic luster, did not change (Table 8) after being exposed to corrosion conditions, but the hardness of the coating slightly increased in 23 days (Table 9). The surface hardness of the coating was measured with the pencil hardness test (Wolff–Wilborn method), which uses pencils of various grades to determine how hard or soft a coating is.

Table 8. Results of changing colors of samples in different corrosion conditions.

Day	Phosphate Steel/Coat			Phosphate Steel with Ce^{3+}/Coat		
	Initial Sample	Humidity Chamber	Immersed in Sea Water	Initial Sample	Humidity Chamber	Immersed in Sea Water
1.	RAL 6013	RAL 6013	RAL 6013	RAL 6013	RAL 6013	RAL 6013
23.	RAL 6013	RAL 6013	RAL 6013	RAL 6013	RAL 6013	RAL 6013

Table 9. Hardness value for medium-hard coatings exposed to different corrosion conditions.

Day	Phosphate Steel/Coat			Phosphate Steel with Ce^{3+}/Coat		
	Initial Sample	Humidity Chamber	Immersed in Sea Water	Initial Sample	Humidity Chamber	Immersed in Sea Water
1.	B	F	HB	HB	F	HB
13.	F	F	-	F	F	-
23.	F	F	F	F	F	F

The measurements of hardness were performed after the samples had been properly dried, respectively after 13 and 23 days. Including the changes in results, surface hardness is still characterized as a medium-hard coating that has a durable film with projected good wear. It is notable that this type of topcoat takes time to develop the appropriate degree of hardness. Theoretically, if coating hardness is increased, the wear and tear resistance of the coating will improve.

3.5. Adhesion Measurements

In this work, dry adhesion of polyurethane and epoxy coatings on phosphated carbon surface and phosphated steel surface with Ce^{3+} ions were measured by the standard pull-off method. The results of the pull-of measurements on the topcoat, for the initial samples and samples exposed to different corrosion conditions, are shown in Table 10. The adhesion forces on phosphated steel samples with polyurethane topcoat were lower than on the coated phosphate steel samples with Ce^{3+} ions. It is therefore difficult to conclude from these results that the phosphatization process affects the increased adhesion of the topcoat.

Table 10. Pull-off adhesion test of the top coating on the phosphate steel and phosphate steel with Ce^{3+} ions: initial state, samples exposed to humidity conditions for 7 days and samples immersed in sea water for 48 h.

	Initial Samples (MPa)	Samples in Humidity Chamber (MPa)	Samples Immersed in 5% NaCl Solution (MPa)
phosphate steel/coat	-	1.67	2.56
	-	-	3.94
phosphated steel with Ce^{3+}/coat	2.59	12.15	4.81
	2.06	12.34	7.31

Due to the loss of adhesion in the intermediate coating, samples did not comply with EN ISO 4624:2016 [35]. A pull stub (dolly) shows a failure in the intermediate coat, which confirms that a chemical bond between epoxy and polyurethane has been accomplished. In this process, cohesive failure within intermediate coat occurs. In the presence of low temperature, epoxy resin did not achieve the appropriate degree of crosslinking as confirmed in Table 10. The intermediate coat was applied in atmospheric conditions at 18.1 °C and relative humidity of 28.9% and dried for 24 h. Theoretically, the curing temperature for polyurethane and epoxy resins is 25 °C.

According to ISO 12944-5 samples were immersed in a 3.5% NaCl solution classified as an Im2 environment. These samples had the lowest results in the pull-off test compared to the samples which had been in the humidity chamber. In other words, the immersed samples at room temperature were exposed to accelerated corrosion unlike samples in the humidity chamber.

Adhesion force shows better results for phosphated samples with Ce^{3+} ions and coat, especially samples which exposed to humidity chamber. An increase in the adhesion force can be caused by increasing temperature and moisture in the humidity chamber. According to EN ISO 6270-2, the samples were exposed to 40 ± 3 °C with 100% of relative

humidity [28]. This temperature had initiated a crosslinking process in the epoxy resin and the hardening of the epoxy in the durometer.

3.6. Electrochemical Impedance Spectroscopy

Simplified Randles circuits were used to describe the electrochemical cell of a metal in an electrolyte. The equivalent circuits consisted of a solution resistance of the NaCl solution, R_s, in a series with an equivalent resistance of the abrasive blasting substrate, R_p, and double layer capacitance, CPE. The constant phase element (CPE) was used to replace the capacitor in the equivalent circuit to fit the impedance characteristic of the double layer more accurately [36]. After the phosphatization process, as shown in Figure 5a, the surface of carbon steel had thin phosphate layer, which is described with $R_{phosphate}$ where R_s is in a series with a parallel combination of an R_p, CPE, and dispersion relation contains (CDC-symbol: O). Due to the very small thickness of the phosphate layer, the phosphate steel sample had a higher value of the R_p and better corrosion resistance, as shown in Table 11. Figure 5b shows ECC models for the phosphate layer with Ce^{3+} ions, a three-layer coating where the electrolyte resistance of NaCl solution (R_s), coat resistance (R_{coat}), and charge transfer resistance (R_p) of corrosion reaction on the steel substrate were calculated. The fitting of the equivalent electric circuit (EEC) modelsfor phosphate steel surface modified with Ni^{2+}, Ce^{3+}, and Ti^{2+} ions and phosphate steel surfaces with Ce^{3+} ions are shown from Figure 6a–h.

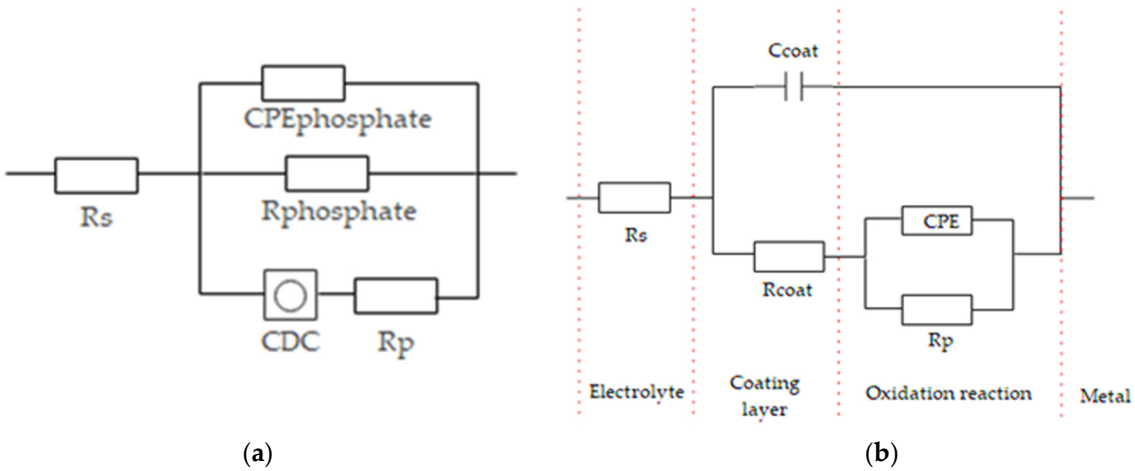

Figure 5. Equivalent electric circuit for fitting EIS parameters for (**a**) phosphate steel surface modified with Ni^{2+}, Ce^{3+}, and Ti^{2+} ions and (**b**) samples with three types of coating [37].

According to Table 11 and Nyquist plot (Figure 6e,f) the phosphating process with Ce^{3+} ion has the best protective and anticorrosion effects. This observation indicates that in this case Ce^{3+} ions were bound on the steel surface which resulted in an increase in the R_p value.

To further study the corrosion resistance of the phosphate layer with Ce^{3+} ions, a three-layer coating system was applied to the samples. The EIS parameters of coatings of the phosphate and phosphate steel surface with Ce^{3+} ions immersed in 3.5 wt.% NaCl solution for 1 h, 14, and 20 days, respectively, are shown in Table 11. Considering the results reported in Table 11, CPE is a constant phase element of the double layer showing its capacitive properties, which depend on the empirical constant n [38]. The value of the constant n is about 1, the CPE can be assumed as the phosphate layer capacitance. Impedance parameters were measured on the topcoat which contained polyurethane. The fitting of equivalent electric circuit models for this system is given in Figure 5b.

Table 11. The results of the EIS measurement on phosphate steel surface and phosphate steel surface modified with Ni^{2+}, Ce^{3+}, and Ti^{2+} ions immediately after different pre-treatment processes immersion in 3.5 wt.% NaCl solution. The table contains the results of EIS measurements for the same samples but with three types of coating respectively after 1-h, 14 and 20 day immersion in 3.5 wt.% NaCl solution.

Samples	R_s (Ω)	CPE_{coat} (F)	n_{coat}	R_{coat} (Ω)	$CPE_{phosphate}$ (F)	$R_{phosphate}$ (Ω)	CPE (F)	R_p (Ω)	Y_o (S·s^5)	B (s^5)
phosphate steel	15.26	-	-	-	9.9×10^{-6}	52.26	9.9×10^{-5}	647.2	3.8×10^{-4}	1.35
phosphate steel with Ni^{2+}	15.31	-	-	-	1.9×10^{-4}	57.3	-	925.1	1.4×10^{-4}	1.25
phosphate steel with Ce^{3+}	15.01	-	-	-	7.9×10^{-4}	901.5	-	1.8×10^{4}	6.6×10^{-5}	1.36
phosphate steel with Ti^{2+}	17.48	-	-	-	7.1×10^{-5}	582.3	-	1.4×10^{3}	1.7×10^{-4}	1.23
immersion after 1 h										
phosphate steel/coat	15.87	5.9×10^{-11}	0.99	1.1×10^{8}	-	-	2.1×10^{-10}	5.4×10^{10}	-	-
phosphate steel with Ce^{3+}/coat	16.34	2.7×10^{-11}	1	3.5×10^{9}	-	-	1.4×10^{-10}	3.6×10^{10}	-	-
immersion after 14 days										
phosphate steel/coat	12.44	3.2×10^{-11}	1	3.9×10^{9}	-	-	8.7×10^{-11}	1.3×10^{11}	-	-
phosphate steel with Ce^{3+}/coat	14.54	1.1×10^{-11}	1	5.9×10^{9}	-	-	3.8×10^{-11}	1.2×10^{11}	-	-
immersion after 20 days										
phosphate steel/coat	17.47	1.2×10^{-11}	1	7.8×10^{9}	-	-	2.3×10^{-10}	1.4×10^{11}		
phosphate steel with Ce^{3+}/coat	15.39	6.4×10^{-12}	1	2.6×10^{10}	-	-	1.1×10^{-11}	3.2×10^{11}	-	-

After a 14-day immersion, epoxy coating and polyurethane showed a good protection effect, and the electrolyte solution did not diffuse on the steel substrate. In fact, the ions were blocked by these organic coatings and were unable to pass through them to the steel surface. After a 480-h immersion in electrolyte, the phosphate steel/coat sample showed a slightly higher value of R_{coat}. This indicated that sparingly soluble salts of zinc phosphate caused the creation of a protective barrier and improved the stability of the epoxy coating. The phosphate carbon steel layer created a mechanical and chemical bond with the coating, as opposed to the bare steel which bonded only mechanically.

According to Figure 7, total resistance (R_t) was calculated with the formula:

$$R_t = R_p + R_{coat} - R_s \quad (3)$$

where the value of resistors is in accordance with the results obtained by EIS for phosphate steel/coat and phosphate steel with Ce^{3+} ions/coat immersion in 3.5 wt.% NaCl solution respectively for 1, 366, and 480 h. The results of this formula are shown in Figure 7. All these anticorrosion properties of the samples gradually increase during the immersion time, which may indicate an improvement in the compatibility between the top and the intermediate coats. Mainly, the values of R_p were very similar for all samples, but phosphate steel with Ce^{3+} ions/coat showed a significant increase after 480 h.

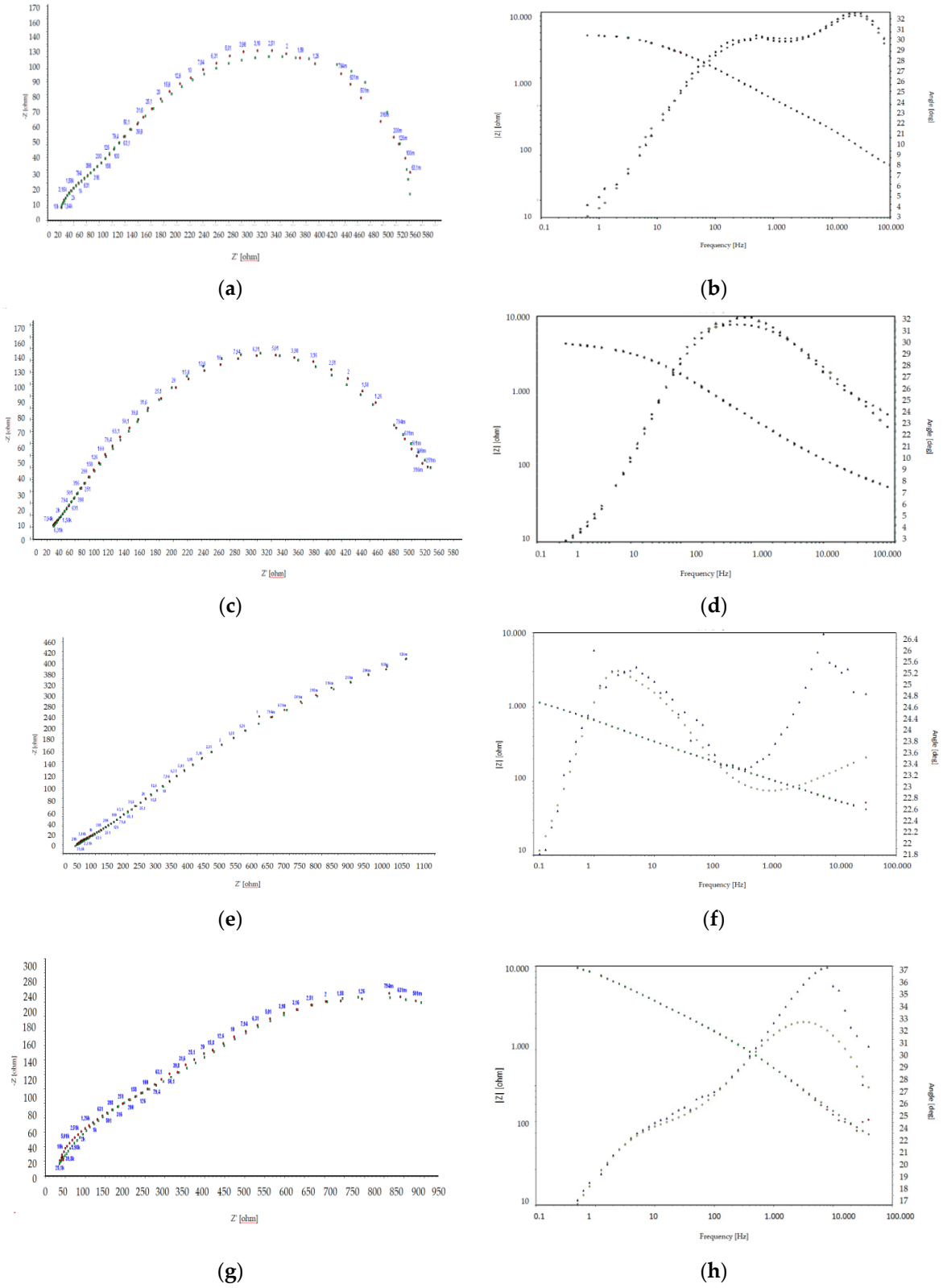

Figure 6. Nyquist and Bode plots and equivalent circuit of the phosphate steel surface (**a**,**b**) and phosphate steel surface with Ni^{2+} ions (**c**,**d**), Ce^{3+} ions (**e**,**f**), and Ti^{2+} ions (**g**,**h**) after 1h immersion in 3.5 wt.% NaCl solution.

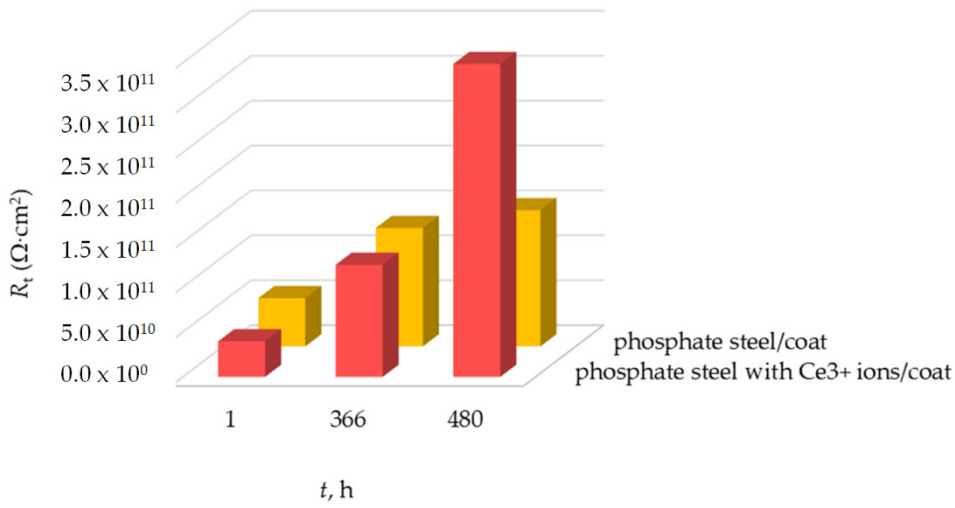

Figure 7. Total resistance value for bare steel/coat and phosphate steel with Ce^{3+}/coat immersion in 3.5 wt.% NaCl solution for 1, 366, and 480 h.

4. Conclusions

Several conclusions can be drawn from this study:

1. Phosphate steel and phosphate steel with Ni^{2+}, Ce^{3+}, and Ti^{2+} ions have the same value of roughness because all samples were prepared with abrasive blasting.
2. All samples show a similar value of thickness and confirm uniformly applied layers.
3. A gray color with a bright metallic luster of samples did not change after being exposed to corrosion conditions.
4. Surface hardness of samples is still characterized as medium-hard, although it takes time for this type of topcoat to develop the appropriate degree of hardness.
5. Due to loss of adhesion in the intermediate coating, samples did not comply with EN ISO 4624:2016. There is no difference in the pull-off values between the phosphate and the phosphate carbon surfaces with Ce^{3+} ions.
6. An analysis of the EIS measurement results showed equal diffusion through all modified layers. Double layer capacitance showed low values, indicating the formation of sparingly soluble phosphate salts on the steel substrate, which results in an increase in the value of R_p and better corrosion protection. Ce^{3+} ions in the form of phosphate salts bind to the carbon steel surface and thus act as an inhibitor for the phosphate surface.
7. After a 20-day immersion, the EIS measurement confirmed that epoxy coating and polyurethane have a good protection effect, and the electrolyte solution had not been diffused on the steel substrate. This is a short period of coating exposure to water penetration, but we can conclude that a long-term corrosion behavior of phosphate carbon steel could offer better corrosion protection due to a significant increase of the R_p value.

Author Contributions: M.S. performed the experiments, analyzed the data and wrote the paper; V.A. designed the experiments and revised the paper, V.Š. analyzed the surface morphology using SEM and EDS spectroscopy. F.K. revised the paper. All authors have read and agreed to the published version of the manuscript.

Funding: This research was funded by "Development of anti-corrosion protection system for multipurpose pipe use" (Grant number: KK.01.1.1.07.0045). This work was supported by the European Regional Development Fund under the Operational Program Competitiveness and Cohesion 2014–2020.

Institutional Review Board Statement: Not applicable.

Informed Consent Statement: Not applicable.

Data Availability Statement: Not applicable.

Acknowledgments: Investigations were performed within the research topic "Development of anti-corrosion protection system for multipurpose pipe use" (Grant number: KK.01.1.1.07.0045).This work was supported by the European Regional Development Fund under the Operational Program Competitiveness and Cohesion 2014–2020.

Conflicts of Interest: The authors declare no conflict of interest.

Abbreviations

The following abbreviations are used in this manuscript:

ISO	International Organization for Standardization
SCE	Saturated calomel electrode
EIS	Electrochemical impedance spectroscopy
CDC	Circuit description code
EEC	Equivalent electric circuit
CPE	Double layer capacitance

References

1. Ubong, M.E.; Mazen, M.K. Corrosion protection of non-alloyed AIAI 316L concrete steel metalgrade in aqueous H_2SO_4. Electro-analytical and surface analyses with Metiamide. *Constr. Build. Mater.* **2014**, *68*, 285–290.
2. Morozov, Y.; Calado, L.M.; Shakoor, R.A.; Kahraman, R.; Taryba, M.G.; Montemor, M.F. Epoxy coatings modified with a new cerium phosphate inhibitor for smart corrosion protection of steel. *Corros. Sci.* **2019**, *159*, 108–128. [CrossRef]
3. Naeem, M.; Shafiq, M.; Zaka-ul-Islamc, M.; Bashir, M.I.; Díaz-Guillénd, J.C.; Lopez-Badilloe, C.M.; Zakaullah, M. Novel duplex cathodic cage plasma nitriding of non-alloyed steel using aluminum and austenite steel cathodic cages. *J. Alloy. Compd.* **2017**, *721*, 307–311. [CrossRef]
4. Francis, R.; Byrne, G. Duplex Stainless Steel–Alloys for the 21st Century. *Metals* **2021**, *11*, 836. [CrossRef]
5. Wang, M.; Wang, J.; Wenbin, H. Preparation and corrosion behavior of Cu-8-HQ@HNTs/epoxy coating. *Prog. Org. Coat.* **2020**, *139*, 105–434. [CrossRef]
6. Finšar, M.; Jackson, J. Application of corrosion inhibitors for steels in acidic media for the oil and gas industry: A review. *Corros. Sci.* **2014**, *86*, 17–41. [CrossRef]
7. López-Ortega, A.; Bayón, R.; Arana, J.L. Evaluation of Protective Coatings for High-Corrosivity Category Atmospheres in Offshore Applications. *Materials* **2019**, *12*, 1325. [CrossRef]
8. Soares, C.G.; Garbatov, Y.; Zayed, A.; Wang, G. Influence of environmental factors on corrosion of ship structures in marine atmosphere. *Corros. Sci.* **2009**, *9*, 2014–2026. [CrossRef]
9. Ramezanzadeh, M.; Ramezanzadeh, B.; Sari, M.G.; Saeb, M.R. Corrosion resistance of epoxy coating on mild steel through polyamidoamine dendrimer-covalently functionalized graphene oxide nanosheets. *J. Ind. Eng. Chem.* **2020**, *82*, 290–302. [CrossRef]
10. Chandler, K.A. *Marine and Offshore Corrosion*; Butterworth-Heinemann: Oxford, UK, 1985; ISBN 978-0-408-01175-4.
11. Silva, E.; Fedel, M.; Deflorian, F.; Cotting, F.; Lins, V. Properties of Post-Consumer Polyethylene Terephtalate Coating Mechanically deposited on Middle Steel. *Coatings* **2019**, *9*, 28. [CrossRef]
12. Khodaei, P.; Shabani-Nooshabadi, M.; Behpour, M. Epoxy-Based nanocomposite coating reinforced by a zeolite complex: Its anticorrosion properties on mild steel in 3.5 wt% NaCl media. *Prog. Org. Coat.* **2019**, *136*, 105–254. [CrossRef]
13. Ramezanzadeh, M.; Ghasem, B.; Ramezanzadeh, B. Development of a nanostructured Ce(III)-Pr(III) film for excellently corrosion resistance improvement of epoxy/polyamide coating on carbon steel. *J. Alloy. Compd.* **2019**, *792*, 375–388. [CrossRef]
14. Zhang, F.; Ju, P.; Pan, M.; Zhang, D.; Yao, D.; Li, G.; Li, X. Self-healing mechanisms in smart protective coatings. *Corros. Sci.* **2018**, *144*, 74–88. [CrossRef]
15. ISO 12944:1-8. *Paints and Varnishes—Corrosion Protection of Steel Structures by Protective Paint Systems*; International Organization for Standardization: Geneva, Switzerland, 2018.
16. Rahmania, P.; Shojaeia, A.; Tavandashti, N.P. Nanodiamond loaded with corrosion inhibitor as efficient nanocarrier to improve anticorrosion behavior of epoxy coating. *J. Ind. Eng. Chem.* **2020**, *83*, 153–163. [CrossRef]
17. Mei, Y.; Xu, J.; Jiang, L.; Tan, Q. Enhancing corrosion resistance of epoxy coating on steel reinforcement by aminobenzoate intercalated layered double hydroxides. *Prog. Org. Coat.* **2019**, *134*, 288–296. [CrossRef]
18. Bajat, J.B.; Mišković-Stanković, V.B.; Popić, J.P.; Dražić, D.M. Adhesion characteristics and corrosion stability of epoxy coatings electrodeposited on phosphate hot-dip galvanized steel. *Prog. Org. Coat.* **2008**, *63*, 201–208. [CrossRef]
19. Alvarado-Macías, G.; Fuentes-Aceituno, J.C.; Salinas-Rodríguez, A.; Rodríguez-Varela, F.J. Understanding the Nature of the Manganese Hot Dip Phosphatizing Process of Steel. *J. Mex. Chem. Soc.* **2013**, *57*, 328–336. [CrossRef]
20. Gang, L.; Wanger, S.; Yanrong, C.; Shili, Z. Quick organic phosphating at room temperature. *Met. Finish.* **1997**, *95*, 54–57.

21. Jegannathana, S.; Sankara Narayanan, T.S.N.; Ravichandran, K.; Rajeswar, S. Formation of zinc phosphate coating by anodic electrochemical treatment. *Surf. Coat. Technol.* **2006**, *200*, 6014–6020. [CrossRef]
22. Jegannathana, S.; Arumugam, T.K.; Sankara Narayanan, T.S.N.; Ravichandran, K. Formation and characteristics of zinc phosphate coatings obtained by electrochemical treatment: Cathodic vs. anodic. *Prog. Org. Coat.* **2009**, *65*, 229–236. [CrossRef]
23. Jiang, C.; Cheng, X. Anti-corrosion zinc phosphate coating on building steel via a facile one-step brushing method. *Electrochem. Commun.* **2019**, *109*, 106596. [CrossRef]
24. Yongsheng, H.; Fuchun, L.; En-Hou, H.; Saima, A.; Guobao, X. The mechanism of inhibition by zinc phosphate in an epoxy coating. *Corros. Sci.* **2013**, *69*, 77–86.
25. Naderi, R.; Attar, M.M. The inhibitive performance of polyphosphate-based anticorrosion pigments using electrochemical techniques. *Dye. Pigment.* **2009**, *80*, 349–354. [CrossRef]
26. ISO 2360. *Non-Conductive Coatings on Non-Magnetic Electrically Conductive Base Metals–Measurement of Coating Thickness–Amplitude-Sensitive Eddy-Current Method*; International Organization for Standardization: Geneva, Switzerland, 2017.
27. Powder Coating Consultants, Machu Test: Accelerated Salt Sprey Test. Available online: https://powdercc.com/pdf/Machu%20Test.pdf (accessed on 8 December 2021).
28. ISO 6270-2. *Paints and Varnishes–Determination of Resistance to Humidity–Part 2: Condensation (In-Cabinet Exposure with Water Reservoir)*; International Organization for Standardization: Geneva, Switzerland, 2017.
29. ISO 8503-1. *Preparation of Steel Substrates before Application of Paints and Related Products–Surface Roughness Characteristics of Blast-Cleaned Steel Substrates–Part 1: Specifications and Definitions for ISO Surface Profile Comparators for the Assessment of Abrasive Blast-Cleaned Surfaces*; International Organization for Standardization: Geneva, Switzerland, 2012.
30. Spahiu, K.; Jordi, B. A selected thermodynamic database for REE to be used in HLNW performance assessment exercises. *Tech. Rep.* **1995**, *28*, 29.
31. Dagdag, O.; El Harfi, A.; El Gana, L.; Hlimi, Z.; Erramli, H.; Hamed, O.; Jodeh, S. The Role of Zinc Phosphate Pigment in the Anticorrosion Properties of Bisphenol A Diglycidyl Ether-Polyaminoamide Coating for Aluminum Alloy AA2024-T3. *J. Bio- Tribo-Corros.* **2018**, *5*, 7. [CrossRef]
32. Zhang, S.; Chen, H.; Zhang, X.; Zhang, M. The growth of zinc phosphate coating on 6061-Al alloy. *Surf. Coat. Technol.* **2008**, *202*, 1674–1680.
33. Hiromoto, S. 3-Chemical solution deposition of hydroxyapatite and octacalcium phosphate coating for magnesium and its alloys to improve biocompatibility. *Woodhead Publ. Ser. Biomater.* **2015**, *2*, 59–80.
34. ASTM B117. *Standard Practice for Operating Salt Spray (Fog) Apparatus*; American Society for Testing and Material: West Conshohocken, PL, USA, 2019.
35. ISO 4624. *Paints and Varnishes–Pull-Off Test for Adhesion*; International Organization for Standardization: Geneva, Switzerland, 2016.
36. Fu, X.; Shen, Z.; Chen, X.; Lin, J.; Cao, H. Influence of Element Penetration Region on Adhesion and Corrosion Performance of Ni-Base Coatings. *Coatings* **2020**, *10*, 895. [CrossRef]
37. Bejinuriu, C.; Burduhos-Nergis, D.-P.; Cimpoesu, N. Immersion Behaviour of Carbon Steel, Phosphate Carbon Steel and Phosphate and Painted Carbon Steel in Saltwater. *Materials* **2021**, *14*, 188. [CrossRef] [PubMed]
38. Stojanović, I.; Šimunović, V.; Alar, V.; Kapor, F. Experimental Evaluation of Polyester and Epoxy-Polyester Polyester Powder Coatings in Aggressive Media. *Coatings* **2018**, *8*, 98. [CrossRef]